J. COMBIN. MATH. COMBIN. COMPUT. 127b (2025) 3429--3442

Journal of Combinatorial Mathematics and Combinatorial Computing
www.combinatorialpress.com/jcmcc

Combinatorial Press

Research on energy optimal control of automation system based on variational approach

Miaoyan Qu[1,✉]

[1] International Engineering College, Shenyang Aerospace University, Shenyang, Liaoning, 110136, China

ABSTRACT

The automation system is gradually applied to many fields because of its intelligent and efficient characteristics, and its energy control makes the equipment work in the optimal efficiency zone, however, the actual control effect needs to be further optimized. This paper explains the energy control problem of automation system for its control process, and uses the weighted residual value method to transform the original system into a system dynamics model. On the basis of this model, the optimal control is solved by the variational method, and the energy control algorithm based on the variational method is built by combining Lie algebra. The algorithm of this paper is used to establish the energy optimal control strategy and simulation experiments are carried out as a prerequisite for constructing the driving cycle. In the simulation experiments, the energy optimal control strategy based on this paper's algorithm saves 4.77% of fuel, which shows that the energy control of the automation system under this paper's algorithm is better and in line with the environmental protection needs.

Keywords: variational method, Lie algebra, energy control algorithm, automated system

1. Introduction

Grid interconnection is the general trend of power system development at home and abroad in recent years, this new situation brings new challenges to the safe and economic operation of the power system, with which the secondary power information system of protection, control, command and control and informatization, automation system must be adapted to the needs of the national network, and adapt to the needs of the market-oriented reform of electricity [1-4]. Power system is a huge primary energy system, responsible for the production, transmission, distribution and use of electricity [5]. If we regard the production, transmission, distribution and use of electric power as a process of movement and change of energy, then the protection, control and command and scheduling of the power system can be regarded as a process of movement and change of power

✉ Corresponding author.
E-mail address: 17769000075@163.com (M. Qu).
Received 15 April 2024; Revised 05 July 2024; Accepted 25 November 2024; Published Online 16 April 2025.
DOI: 10.61091/jcmcc127b-191

information [6-7]. Throughout the development of power dispatch automation system, the initial stage for the monitoring and control and data collection system, and then gradually increased the power generation control, economic scheduling and security analysis and other functions, and in recent years in the system design and development of the introduction of network and communication technology, distributed computer technology and other modern information technology, the latest achievements, the development of today's energy management system (EMS) [8-12].

The introduction of computer network technology has led to a significant development of the EMS architecture, and the traditional dispatch center has evolved into an open and distributed modern energy control center [13-15]. The modern energy control center is no longer a simple grid operation monitoring center, which is not only responsible for safety and operation, but also for trading and operation, and is a highly informatized, intelligent, integrated and automated command and decision-making center on behalf of the entire electric power enterprise to achieve power dispatch, management and operation of the power system [16-19]. The modern energy control center is characterized by a high degree of informatization, intelligence, integration and automation [20]. And with the rapid development of information technology, modern energy control centers are able to achieve optimal control of energy in automation systems through digital technology [21].

This paper describes the energy control problem in mathematical form as a premise, and equates the energy control of automation system to a system dynamics model. Based on this model, the variational method is introduced as the solution method of optimal control, and Lie algebra is integrated to build the energy control algorithm of automation system based on the variational method. Then integrate and extract the optimal solution of this paper's algorithm for hybrid mining trucks, construct the energy management strategy based on the optimal control rules, and carry out simulation experiments at the same time. Under the guidance of the energy optimal control strategy of this paper's algorithm, the driving cycle is constructed.

2. Analysis and modeling of energy control

The construction of the mathematical model of the automated system is the basis of this research and the key to design and improve the energy control. This chapter analyzes the energy control problem from a mathematical point of view and constructs a mathematical theoretical model for energy control of automated systems.

2.1. Description of the energy control problem

The study of transient optimal energy control strategy in this paper is based on a single-axis parallel hybrid hybrid powertrain, and Fig. 1 shows the structural layout of the hybrid powertrain.

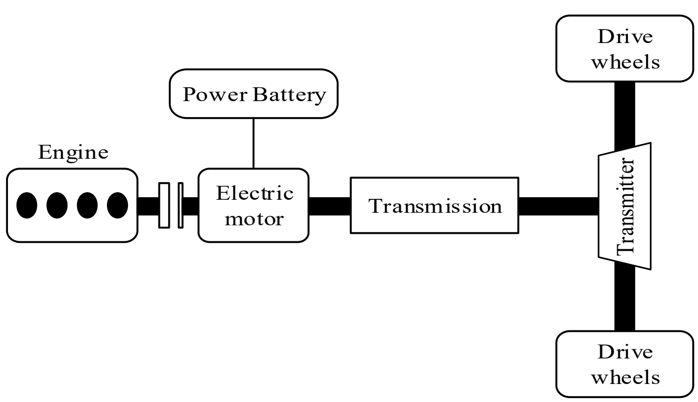

Fig. 1. Structure layout of single-axis parallel hybrid power system

The coaxial arrangement of the engine and the motor requires that the two in must have the same rotational speed, and the sum of the torque of the two must be equal to the demand torque at the input of the gearbox, as in equations (1) and (2):

$$w_e(t) = w_m(t) = w_g(t) \tag{1}$$

$$T_{tot}(t) = T_e(t) + T_m(t) \tag{2}$$

where w_e, w_m and w_g represent the engine speed, motor speed and gearbox input speed respectively. T_e, T_m, and T_{tot} represent the engine torque, motor torque, and transmission input torque values, respectively.

The study of the energy control strategy is mainly to determine in what proportion the demanded torque of the system should be distributed between the engine and the electric motor at each instant, so as to minimize the fuel consumption or the pollutant emission of the vehicle during the whole driving process. In this paper, the study of the energy control strategy of the hybrid powertrain is focused on achieving the best fuel economy, so the cost function of the energy control of the system is given in equation (3):

$$J = \int_0^T \dot{m}_e\left(P_e(t)\right)dt \tag{3}$$

As shown in Eq. (4), the optimal energy control strategy of the hybrid power system is to make the cost function obtain the minimum value by the rational allocation of energy at each time step. At the same time, the solution of the energy control problem is subject to the limitations and constraints of a variety of conditions as shown in Eqs. (5)-(8).

$$\left\{P_e^{opt}(t), P_m^{opt}(t)\right\} = \arg \min_{\{P_e(t), P_m(t)\}} Jt = 0 \ldots T \tag{4}$$

$$P_{tot}(t) = P_e(t) + P_m(t) \tag{5}$$

$$SOC_{\min} \le SOC(t) \le SOC_{\max} \tag{6}$$

$$0 \le P_e(t) \le P_{e,\max}(t) \tag{7}$$

$$P_{m,mix}(t) \le P_m(t) \le P_{m,\max}(t) \tag{8}$$

2.2. System dynamics modeling

The mechanical model considered in this paper consists of two parts: the linear main structure and the NES device attached to it. The main structure mass m_1 is attached to the ground through linear damping c_1 and linear stiffness k_1. The NES device consists of a small mass block m_2, three times nonlinear stiffness k_2 and linear damping c_2. The specific structure of the model is shown in Fig. 2.

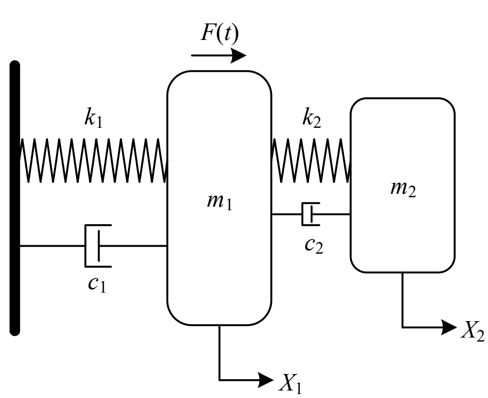

Fig. 2. A SDOF system coupled with NES device

By considering the dynamic equilibrium conditions and the coupling between the main structure and the NES, the differential equation of motion for this system is given by equation (9):

$$\begin{cases} m_1\ddot{X}_1 + c_1\dot{X}_1 + k_1X_1 + c_2\left(\dot{X}_1 - \dot{X}_2\right) + \\ k_2\left(X_1 - X_2\right)^3 = F(t) \\ m_2\ddot{X}_2 + c_2\left(\dot{X}_2 - \dot{X}_1\right) + k_2\left(X_2 - X_1\right)^3 = 0 \end{cases} \tag{9}$$

where: X_1 and X_2 are the displacement response of the main structure and the NES relative to the ground, respectively. $F(t)$ is the external excitation acting on the main structure of the system.

To simplify the derivation, the dimensionless parameters: $\varepsilon = m_2 / m_1$, $\lambda_1 = c_1 / m_1$, $\lambda_2 = c_2 / \varepsilon m_1$, $\omega_0^2 = k_1 / m_1$, $k_n = k_2 / m_1$, $\xi(t) = F(t) / m_1$ are introduced and substituted into Eq. to obtain Eq. (10):

$$\begin{cases} \ddot{X}_1 + \varepsilon\lambda_1\dot{X}_1 + \omega_0^2X_1 + \varepsilon\lambda_2\left(\dot{X}_1 - \dot{X}_2\right) + \\ k_n\left(X_1 - X_2\right)^3 = \xi(t) \\ \varepsilon\dot{X}_2 + \varepsilon\lambda_2\left(\dot{X}_2 - \dot{X}_1\right) + k_n\left(X_2 - X_1\right)^3 = 0 \end{cases} \tag{10}$$

where $\xi(t)$ is a zero-mean Gaussian process of intensity $2D$ satisfying $E[\xi(t)\xi(t+\tau)] = 2D\delta(\tau)$, $E(\cdot)$ is the mathematical expectation, and $\delta(\tau)$ is the Diracdelta function.

The new variable Eq. (11) is now introduced:

$$u_1 = X_1 + \varepsilon X_2, u_2 = X_1 - X_2 \tag{11}$$

where u_1 and u_2 are the center of mass displacement and relative displacement, respectively. Combining Equation (10), an equivalent system about u_1 and u_2 can be obtained. The result is equation (12):

$$\begin{cases} \ddot{u}_1 + C_1\dot{u}_1 + C_2u_1 + C_3\dot{u}_2 + C_4u_2 = \xi(t) \\ \ddot{u}_2 + C_5\dot{u}_2 + C_6u_2^3 + C_1\dot{u}_1 + C_2u_1 + C_4u_2 = \xi(t) \end{cases} \tag{12}$$

where $C_i (i = 1, 2, \cdots, 6)$ is specifically expressed as in equation (13):

$$\begin{aligned} &C_1 = \frac{\varepsilon\lambda_1}{1+\varepsilon}, C_2 = \frac{\omega_0^2}{1+\varepsilon}, C_3 = \frac{\varepsilon^2\lambda_1}{1+\varepsilon} \\ &C_4 = \frac{\varepsilon\omega_0^2}{1+\varepsilon}, C_5 = (1+\varepsilon)\cdot\lambda_2 + C_3, C_6 = \left(k_n + \frac{k_n}{\varepsilon}\right) \end{aligned} \tag{13}$$

Now, by noting $Q_1 = u_1$, $P_1 = \dot{u}_1$, $Q_2 = u_2$, $P_2 = \dot{u}_2$, the Ito stochastic differential equation of Eq. (12) can be written directly as Eq. (14):

$$\begin{gathered} dQ_1 = P_1dt \\ dP_1 = \left(-C_1P_1 - C_2Q_1 - C_3P_2 - C_4Q_2\right)dt + \sqrt{2D}dB(t) \\ dQ_2 = P_2dt \\ dP_2 = \left(-C_5P_2 - C_6Q_2^3 - C_1P_1 - C_2Q_1 - C_4Q_2\right)dt + \sqrt{2D}dB(t) \end{gathered} \tag{14}$$

where $B(t)$ is the unit Wiener process.

The smooth FPK equation for the steady state probability density function ρ governing the system Eq. (14) is Eq. (15):

$$-\frac{\partial(m_1\rho)}{\partial q_1}-\frac{\partial(m_3\rho)}{\partial q_2}-\frac{\partial(m_2\rho)}{\partial p_1}-\frac{\partial(m_4\rho)}{\partial p_2} \\ +\frac{D\dot{\partial}^2\rho}{\partial p_1^2}+\frac{2D\partial^2\rho}{\partial p_1\partial p_2}+\frac{D\partial^2\rho}{\partial p_2^2}=0 \tag{15}$$

where $m_i(i=1,2,\cdots,4)$ is equation (16), respectively:

$$m_1=p_1, m_2=-C_1p_1-C_2q_1-C_3p_2-C_4q_2m_3=p_2, m_4 \\ =-C_5p_2-C_6q_2^3-C_1p_1-C_2q_1-C_4q_2 \tag{16}$$

The exact smooth solution of equation (15) is not available in general. In addition, the high dimensionality of the equations requires a large amount of computation and data storage for direct numerical solution, and numerical methods such as the finite difference method are not suitable for parameter optimization and analysis studies of NES. In this paper, a weighted residual minimization technique based on the FPK equations of the original system and the FPK equations of the equivalent system is proposed to find the approximate analytical expressions of the smooth solutions of the original system for the purpose of NES parameter optimization analysis.

3. Energy control algorithm based on the variational method

Based on the mathematical model established in Chapter 2, this chapter details the principle and process of solving the optimal control by the variational method, and combines with Lie algebra to construct an energy control algorithm based on the variational method as a solution algorithm for the optimal control of energy in automation systems.

3.1. Variational methods and optimal control

The calculus of variations is a branch of mathematics that was gradually formed and developed at the end of the 17th century. It is a classical method to study the generalized function extremum, and it has a wide range of applications in many fields of natural science. The optimal control problem is a kind of generalized function extreme value problem, so the variational method is an important tool to study the optimal control problem.

1) Propose the optimal control problem. A practical optimal control problem is always an optimal treatment of a process, so it possesses initial conditions, system equations, objective set, control domain, and performance function of the system. The expression (17) is given below:

$$\begin{cases} X(t_0)=X_0 & \text{Initial conditions} \\ \dot{X}=f(x(t),x(t),t) & \text{System equations} \\ J=K(x(T),T)+\int_{t_0}^{T}L(x(t),u(t),t)dt & \text{Performance indicators} \\ U & \text{Control domain} \\ S & \text{Target set} \end{cases} \tag{17}$$

2) Equation of state of a system. The equation of state connects the expressions for the inputs and states of the system and is the basis for dealing with multiple-input-multiple-output problems, and the computational formula (18) for establishing the equation of state is given below:

$$f(x(t),u(t),t)-\dot{x}(t)=0 \tag{18}$$

3) Establishment of performance index function. A good control system needs to establish a performance indicator function with good robustness based on various control action sets, so as to optimally control the system, using Lagrange multipliers to bring the conditional equation into the indicator to get the equivalent performance indicator function as in Eq. (19):

$$J_I = K(x(T),T) + \int_{t_0}^{T} [L(x(t),u(t),t + \lambda(f(x,u,t) - \dot{x})]dt \tag{19}$$

Hamiltonian function is an extension of classical calculus of variations, using regular equations to describe the system formed by the motion, suitable for dynamic optimization of the system, the introduction of the Hamiltonian function, the original conditional extrema, is transformed into the problem of finding the unconditional extrema of the generalized function J_1. For convenience, the introduction of a scalar function, called $H(x,u,\lambda,t)$ for the Hamiltonian function as in equation (20):

$$H(x,u,\lambda,t) = L(x,u,t) + \lambda^T f(x,u,t) \tag{20}$$

4) Solve the optimal solution set. Since the objective function is relatively simple, without considering the influence of extreme values and boundaries, the variational method uses the idea of the derivative to solve the maximum and minimum value of the function, and the problem is solved on the basis of Eq. (21)-(22):

$$\text{The condition satisfied by the minimal value of J is: } \begin{cases} \delta J = 0 \\ \delta^2 J > 0 \end{cases} \tag{21}$$

$$\text{The condition satisfied by the extremely large value of J is: } \begin{cases} \delta J = 0 \\ \delta^2 J > 0 \end{cases} \tag{22}$$

This leads to the optimal control conditions for the variational method in a certain time domain, $x^*(t)$, $\lambda^*(t)$ satisfy the canonical equation (23), and $x^*(t)$, $\lambda^*(t)$ satisfy the endpoint condition equation (24):

$$\dot{x}(t) = \left.\frac{\partial H}{\partial \lambda}\right|_*, \dot{\lambda}^*(t) = -\left.\frac{\partial H}{\partial x}\right|_* \tag{23}$$

$$\dot{x}^*(t_0) = x_O, \lambda^*(T) = \left.\frac{\partial K}{\partial x(T)}\right|_* \tag{24}$$

The Hamiltonian function rewritten by the performance index function, in dynamic control, needs to satisfy certain conditions, Eq. (25) gives the expression of the Hamiltonian function, Eq. (26) denotes H about the condition that the optimal control has a stabilizing value, and Eq. (27) is the optimal trajectory:

$$H = L(x,u,t) + \lambda^T f(x,u,t) \tag{25}$$

$$\left.\frac{\partial H}{\partial u}\right|_* = 0 \tag{26}$$

$$H^*(t) = H^*(T) - \int_t^T \left.\frac{\partial H}{\partial t}\right|_* dt \tag{27}$$

The above conditions are given as necessary conditions for optimal control, for practical problems, if the optimal control exists and there is a unique solution with the above necessary conditions, then this solution is the optimal control.

3.2. Lie algebra calculus of variations

The vector ω in the kinetic energy becomes the form of the antisymmetric matrix $S(\omega)$. From the concept of Lie algebra, define R as an exponential form as in equation (28):

$$R^{\varepsilon} = \mathrm{R}e^{\varepsilon S(\eta)} \tag{28}$$

where ε is an infinitesimal variable, η is a three-dimensional variational vector, and $S(\eta)$ is an antisymmetric array. The variational differentiation of R can be regarded as the differentiation of the infinitesimal quantity ε as in Eq. (29):

$$\delta \mathbf{R}^{\varepsilon} = \left.\frac{d}{d\varepsilon}\right|_{\varepsilon=0} \mathbf{R}e^{\varepsilon S(\eta)} = \mathbf{R}S(\eta) \tag{29}$$

According to the nature of the exponential matrix, Eq. (28) is expanded into Eq. (30):

$$R^{\varepsilon} = R + \varepsilon RS(\eta) + \mathrm{O}\left(\varepsilon^2\right) \tag{30}$$

Derivation of equation (30) leads to equation (31):

$$\dot{R}^{\varepsilon} = \dot{R} + \varepsilon \dot{R}S(\eta) + \varepsilon RS(\dot{\eta}) \tag{31}$$

From Eq. $S\left(\omega^{\varepsilon}\right) = R^{ET}\dot{R}^{\varepsilon}$, Eq. (30) and Eq. (31) can be obtained from Eq. (32) by bringing Eq. (30) and Eq. (31) into $S\left(\omega^{\varepsilon}\right)$ and omitting $\mathrm{O}\left(\varepsilon^2\right)$:

$$\begin{aligned} S\left(\omega^{\varepsilon}\right) = & S(\omega) + \varepsilon S(\dot{\eta}) + \varepsilon S(\omega)S(\eta) \\ & -\varepsilon S(\eta)S(\omega) \end{aligned} \tag{32}$$

The Lie algebraically transformed form of the $tr[*]$-part is obtained from Eq. (32), retaining the term with coefficient ε as Eq. (33):

$$\begin{aligned} S\left(\omega^{\varepsilon}\right)J_d S^T\left(\omega^{\varepsilon}\right) = & -\varepsilon S(\omega)J_d S(\eta) \\ & +\varepsilon S(\omega)J_d S(\eta)S(\omega) - \varepsilon S(\eta)J_d S(\omega) \\ & -\varepsilon S(\omega)\left[J_d S(\omega)S(\eta) + S(\eta)J_d S(\omega)\right] \\ & +\varepsilon S(\eta)S(\omega)J_d S(\omega) \end{aligned} \tag{33}$$

As a result, the variation on the Lie group becomes a variation on the Lie algebra as in Eq. (34):

$$\begin{aligned} \delta B = & \left.\frac{d}{d\varepsilon}\right|_{s=0} \int_{t_0}^{t_f} L(b,\dot{b},R,\omega)dt \\ = & \int_{t_0}^{t_f}\left[\left.\frac{d}{d\varepsilon}\right|_{\varepsilon=0} L(b,\dot{b},R,\omega)\right]dt \end{aligned} \tag{34}$$

Expanding Eq. (34) and calculating gives Eq. (35):

$$\begin{aligned} \left.\frac{d}{d\varepsilon}\right|_{\varepsilon=0} L(b,\dot{b},R,\omega) = & tr\left[mgS(\eta)R^T e_3^T r\right] \\ & -1/2tr\left\{S(\eta)\left[S(\omega)J_d + J_d S(\omega)\right]\right\} \\ & +1/2tr\left\{S(\eta)S(\omega)\left[S(\omega)J_d + J_d S(\omega)\right]\right\} \\ & -1/2tr\left\{S(\eta)\left[S(\omega)J_d + J_d S(\omega)\right]S(\omega)\right\} \end{aligned} \tag{35}$$

Eqs. $mge_3^T RS(\eta)r = tr\left[mge_3^T RS(\eta)r\right]$, J, ω, and J_d are related to each other by the following equation (36):

$$S(J\omega) = S(\omega)J_d + J_d S(\omega) \tag{36}$$

Eq. (36) is brought into Eq. (35) and collapsed to give Eq. (37):

$$\left.\frac{d}{d\varepsilon}\right|_{\varepsilon=0} L(b,\dot{b},R,\omega) = tr\left[S(\eta)mgR^T e_3^T r\right] + \frac{1}{2} tr\{S(\eta)S(\omega\times J\omega) - S(\eta)S(J\omega)\} \tag{37}$$

Eq. $S(x\times y) = S(x)S(y) - S(y)S(x)$.

4. Application of algorithms and experiments

In order to test the effectiveness of the algorithms in this paper, hybrid vehicles equipped with automation systems are selected as the research object in this chapter to carry out the research on the energy optimal control strategy. The energy management strategy is the core of the efficient operation of hybrid vehicles based on automation systems, and it is also the key to the energy control of hybrid vehicles. In this chapter, the energy optimal control strategy based on the algorithm of this paper is firstly established, and the effectiveness of the strategy is verified by simulation experiments. Then the driving cycle based on this paper's algorithm is constructed as the basis for the practical application of this paper's algorithm.

4.1. Algorithmic energy-optimal control strategy

The energy management strategy based on the algorithm in this paper can obtain the global optimal solution, however, its online application is limited by its large computational volume and the need to predict the driving conditions. In order to realize the real-time control of the energy management strategy based on the algorithm of this paper, its optimal solution is integrated. Taking the hybrid mining truck as an example, each operating mode is calibrated, and the boundaries of the operating modes are extracted to obtain the optimal control rules, so as to establish the energy management strategy based on the optimal control rules under the algorithm of this paper. Simulation experiments of this energy management strategy are also carried out to verify its effectiveness.

4.1.1. Optimal Solution Integration and Working Mode Calibration. The hybrid system of an ordinary hybrid vehicle generally has seven operating modes, i.e., motor drive mode, engine drive mode, engine drive and energy storage mode, combined drive mode, regenerative braking mode, mechanical braking mode, and parking mode. Fig. 3 shows the torque distribution curve based on the energy management strategy of the algorithm in this paper, and it can be found that the hybrid mining truck does not have a combined drive mode and an engine-driven with energy storage mode. This is because considering the special characteristics of the working environment of the hybrid mining truck, this paper retains the prototype engine in case of power battery failure can still maintain the power performance of the prototype, so there is no joint drive mode, but there is a prototype drive mode. And because of the special characteristics of the hybrid mining truck driving conditions, so there is also no engine drive and energy storage mode.

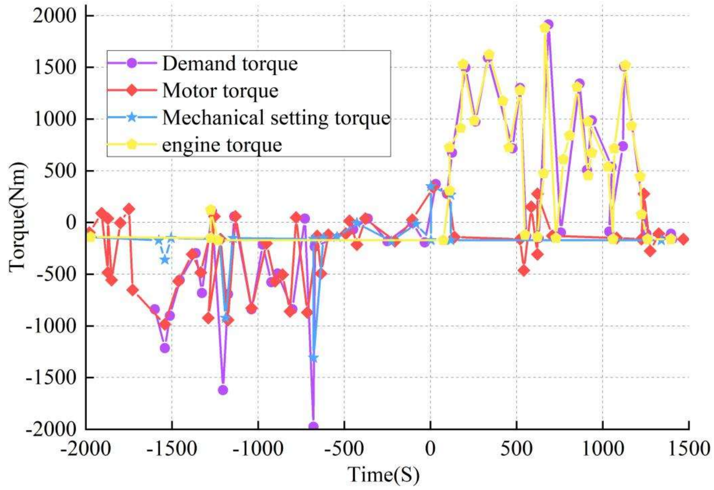

Fig. 3. Torque distribution curve

The working mode distribution points are obtained through the above calibration conditions are shown in Fig. 4, including SOC-vehicle speed plane points, SOC-demand torque plane points and demand torque-vehicle speed plane points. The delineation results are differentiated by working points with different colors and shapes, so as to extract the optimal boundary, i.e., the optimal control rule, and design the energy management strategy based on the optimal control rule under the algorithm of this paper.

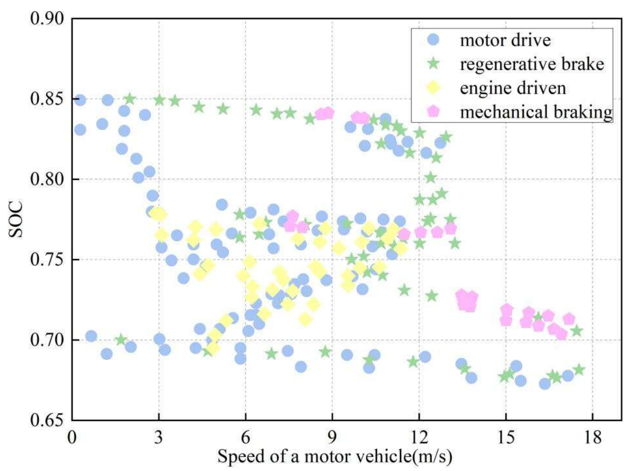

(a) SOC- Speed plane point

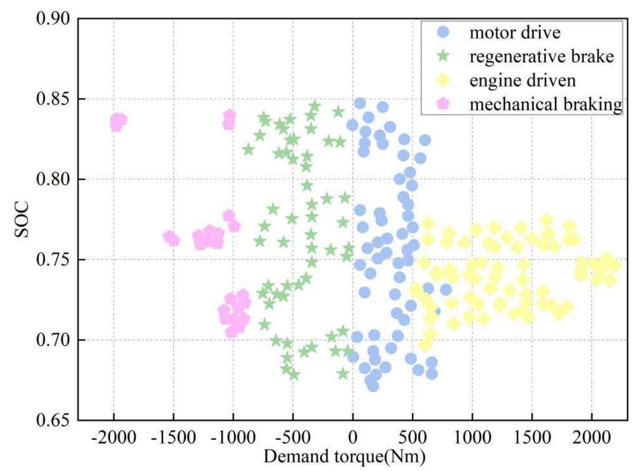

(b) SOC- demand torque plane point

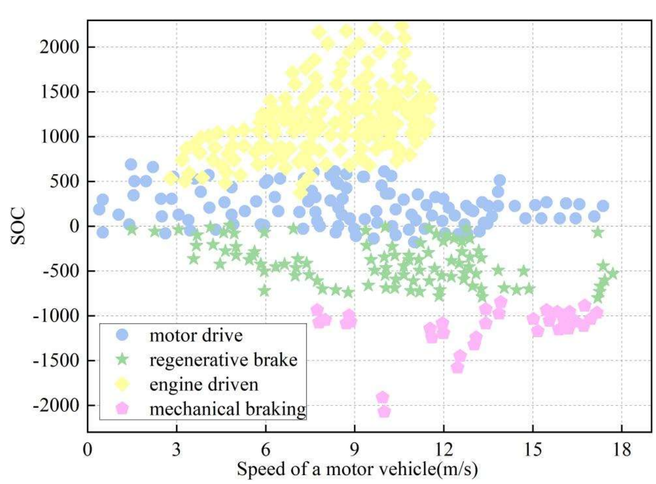

(c) Demand torque - speed plane point

Fig. 4. Work mode distribution point

4.1.2. Simulation experiments. A plug-in hybrid vehicle simulation model is constructed in the form of Cruise and Simulink co-simulation, and the simulation experiment of the energy management strategy based on the optimal control rule of the algorithm in this paper is carried out.

The simulation curve adopts the C-WTVC dump truck regulatory working conditions, the total length of 400s simulation time, the simulation requirements are as follows: the vehicle dynamics, vehicle speed following judgment standard refers to the GB 27840 standard——— speed deviation should not exceed ±3km/h, each time the speed deviation time should not exceed 2s, and the cumulative should not exceed 10s. The SOC change rate of battery charge under one driving cycle condition is <0.1%. Simulation resistance mode with Function without Reference Vehicle. C-WTVC working conditions - based on this paper's algorithm strategy SOC change curve is shown in Figure 5.

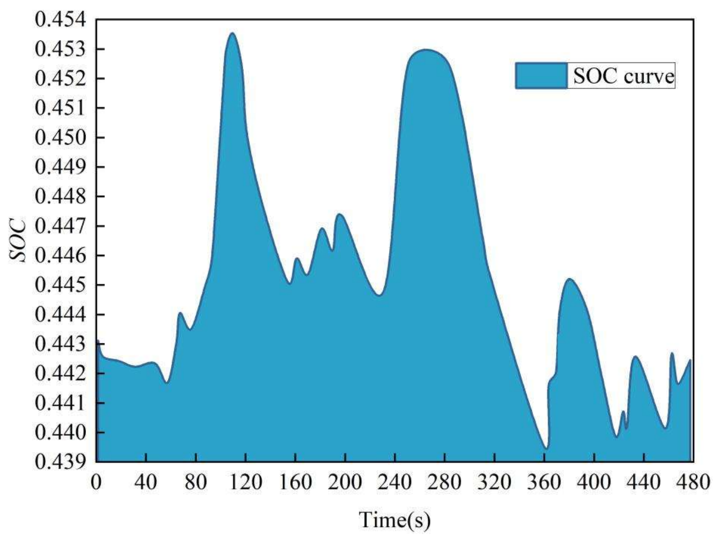

Fig. 5. SOC curve of C-WTVC working condition and Textual algorithm strategy

From Fig. 5, it can be seen that running the whole working condition, the SOC changes from the initial value of 44.3% to 44.21%, and the SOC change rate is about 0.02%, which meets the simulation requirements.

The fuel consumption percentage distribution of the energy management strategy based on the algorithm of this paper is shown in Fig. 6.

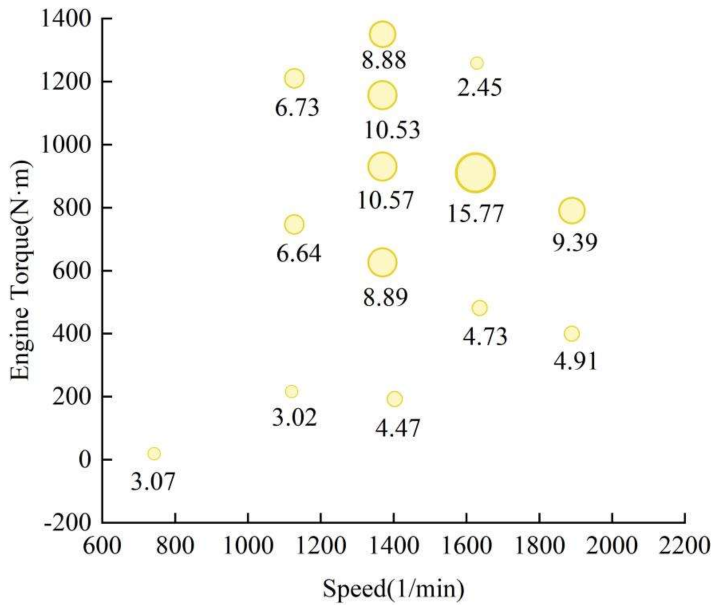

Fig. 6. ECMS control strategy - Fuel consumption ratio distribution

The percentage distribution of torque greater than 1200N-m and in Figure 6 is small, that is to say, it shows that the demand load distribution is in the percentage of the engine high efficiency zone, and the energy management strategy of this paper's algorithm is better controlled and more fuel-efficient. According to the simulation calculation the fuel saving rate of this strategy is 4.78%. As mentioned above, the speed following under the energy management strategy of this paper's algorithm meets the regulatory requirements and satisfies the requirement that the change rate of battery power SOC under one driving cycle condition is <0.1%.

4.2. Driving cycle construction based on the algorithm in this paper

This section centers on the process of constructing driving cycles (SODCs) for specific driving scenarios, and generates SODCs for specific driving scenarios by using the algorithms in this paper, which serves as a strong reference for the practical application of the algorithms in this paper.

4.2.1. Scene Analysis. Logistics and transportation scenarios as the main scenarios of heavy-duty hybrid vehicle operation, driving roads are mainly highways, national highways, and some even contain part of the mountain roads and off-road driving scenarios, the whole vehicle starting and stopping conditions account for a relatively small number of one-way short trip segments last is often longer. This subsection selects the heavy commercial vehicles running in a province and its nearby areas as the basis of the Vehicle Network Driving Data (VND) to construct the SODC for logistics transportation scenarios.

The slope change of the logistics transportation driving scenario after the value-added slope data is shown in Fig. 7, and it can be seen that the slope change is large in this driving scenario, with nearly half of the driving conditions having slopes of more than ±5%, and some of them reaching about ±10%, and even some of them reaching about ±20%, which is due to the fact that the logistics transportation scenario contains a lot of intercity and even inter-provincial transportation conditions, which involves the problem of cross-topography driving, and contains a lot of mountainous areas, and also contains a lot of mountainous areas. This is due to the fact that the logistics transportation scenario contains many intercity and even inter-provincial transportation conditions, which involves cross-terrain driving, and contains more mountainous transportation conditions. In addition, the change of vehicle weight in this scenario is often large, and the difference between fully loaded and unloaded vehicle weight can sometimes be ten times, so the impact of the change of vehicle weight cannot be ignored when upgrading the power system and optimizing the energy management strategy. After the short trip segmentation, it is found that there are short trip segments with too long duration in this scenario, for example, the longest short trip segment in the selected dataset has a duration of 9,549 s, which also matches with the driving scenario of logistic transportation, and if the short trip splicing method is adopted, it will result in the final construction of the SODC being too long, which is not able to meet the needs of the project.

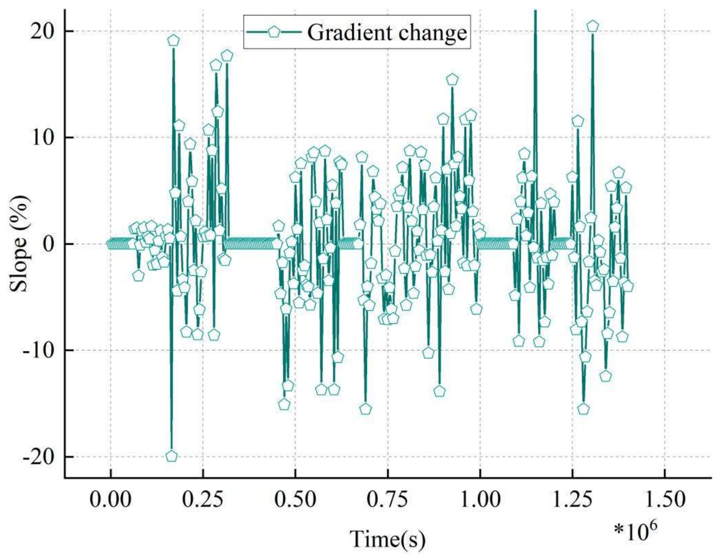

Fig. 7. The gradient change of logistics transportation driving scenario

In summary, when constructing SODC for logistics and transportation scenarios, we should select high-dimensional state variables related to vehicle speed and torque demand, such as vehicle speed, gradient and vehicle weight, and try to use the energy-optimal control algorithm based on the variational method to start the construction.

4.2.2. SODC generation. Once the TPM modeling for each driving pattern is completed, a random number generator is utilized to implement the algorithm of this paper for loop generation. Driving cycles of arbitrary durations can be generated when using the generative method to construct cycles. In order to determine the optimal loop duration, the SODCs using a duration of 2000 s to 14000 s were compared, respectively, and the eigenvalue deviations of the SODCs corresponding to different durations from the original data are shown in Table 1.

Table 1. Deviation from the original driving cycle for different duration candidates

Duration (s)	2500	5500	8500	10500	12500	15500
average velocity speed	30.8	28.08	27.53	25.01	30.33	23.25
Standard deviation of vehicle speed	3.39	7.73	7.39	3.28	2.832	7.21
Maximum speed	19.7	13.97	22.98	12.98	22.01	12.37
Maximum positive acceleration	44.7	44.5	35.16	35.14	44.62	35.47
Maximum negative acceleration	47.4	42.3	42.23	37.05	26.49	37.04
Acceleration standard deviation	19.9	-18.35	18.54	17.57	23.37	16.66
average power	13.14	-27.5	23.39	9.54	25.18	13.17
Power standard deviation	0.5	13.9	17.34	1.43	9.77	3.07
maximum power	6.9	13.7	9.11	1.138	3.78	1.52
MAF	21.44	3.16	3.71	18.46	4.46	9.93

Considering the computational efficiency and expressive ability, the SODC of 10000s was finally selected as the driving cycle for subsequent training is shown in Fig. 8, in which the duration of the three driving modes were 1800s, 350s and 7800s, respectively.

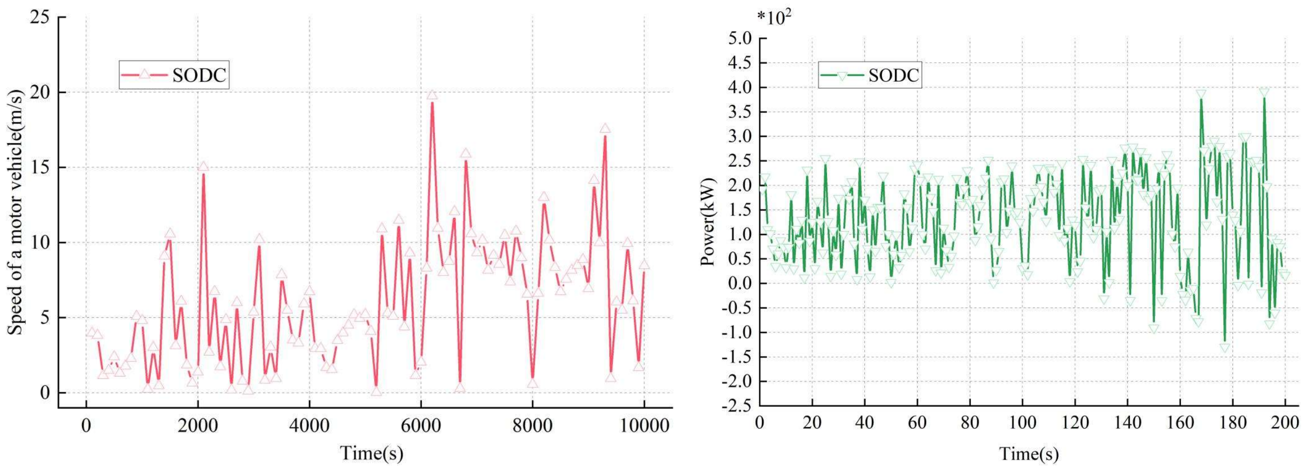

(a) Speed change (b) Power variation

Fig. 8. SODC for logistics transportation scenarios

5. Conclusion

The research conclusions of this paper are as follows:

1) Construct a mathematical model by analyzing the energy control problem of the automation system, integrate the variational method and Lie algebra to form an energy control algorithm based on the variational method, so as to realize the solution of the optimal control of the energy of the automation system.

2) Simulation experiments are carried out while obtaining the energy management strategy based on the optimal control rules of this paper's algorithm, in which the change rate of battery lighting SOC is about 0.02%, and the fuel saving rate is as high as 4.77%, which not only has a better energy control effect but also has a higher fuel saving rate, which proves the feasibility and validity of this paper's algorithm in the optimal control of energy.

References

[1] Heidari, S., Fotuhi-Firuzabad, M., & Lehtonen, M. (2017). Planning to equip the power distribution networks with automation system. IEEE Transactions on Power Systems, 32(5), 3451-3460.

[2] Sajadi, A., Strezoski, L., Strezoski, V., Prica, M., & Loparo, K. A. (2019). Integration of renewable energy systems and challenges for dynamics, control, and automation of electrical power systems. Wiley Interdisciplinary Reviews: Energy and Environment, 8(1), e321.

[3] Kulkarni, V., Sahoo, S. K., Thanikanti, S. B., Velpula, S., & Rathod, D. I. (2021). Power systems automation, communication, and information technologies for smart grid: A technical aspects review. TELKOMNIKA (Telecommunication Computing Electronics and Control), 19(3), 1017-1029.

[4] Sayed, K., & Gabbar, H. A. (2017). SCADA and smart energy grid control automation. In Smart energy grid engineering (pp. 481-514). Academic Press.

[5] Arani, A. K., Gharehpetian, G. B., & Abedi, M. (2019). Review on energy storage systems control methods in microgrids. International journal of electrical power & energy systems, 107, 745-757.

[6] Li, X., & Wang, S. (2019). Energy management and operational control methods for grid battery energy storage systems. CSEE Journal of Power and Energy Systems, 7(5), 1026-1040.

[7] Akram, U., Nadarajah, M., Shah, R., & Milano, F. (2020). A review on rapid responsive energy storage technologies for frequency regulation in modern power systems. Renewable and Sustainable Energy Reviews, 120, 109626.

[8] Abele, E., Panten, N., & Menz, B. (2015). Data collection for energy monitoring purposes and energy control of production machines. procedia CIRP, 29, 299-304.

[9] Ullah, K., Basit, A., Ullah, Z., Aslam, S., & Herodotou, H. (2021). Automatic generation control strategies in conventional and modern power systems: A comprehensive overview. Energies, 14(9), 2376.

[10] Li, Q., Gao, D. W., Zhang, H., Wu, Z., & Wang, F. Y. (2017). Consensus-based distributed economic dispatch control method in power systems. IEEE transactions on smart grid, 10(1), 941-954.

[11] Mahmoud, M. S., Alyazidi, N. M., & Abouheaf, M. I. (2017). Adaptive intelligent techniques for microgrid control systems: A survey. International journal of electrical power & energy systems, 90, 292-305.

[12] Rathor, S. K., & Saxena, D. (2020). Energy management system for smart grid: An overview and key issues. International Journal of Energy Research, 44(6), 4067-4109.

[13] Rafique, S. F., & Jianhua, Z. (2018). Energy management system, generation and demand predictors: a review. IET Generation, Transmission & Distribution, 12(3), 519-530.

[14] Zahraoui, Y., Alhamrouni, I., Mekhilef, S., Basir Khan, M. R., Seyedmahmoudian, M., Stojcevski, A., & Horan, B. (2021). Energy management system in microgrids: A comprehensive review. Sustainability, 13(19), 10492.

[15] Zhao, B., Wang, X., Lin, D., Calvin, M. M., Morgan, J. C., Qin, R., & Wang, C. (2018). Energy management of multiple microgrids based on a system of systems architecture. IEEE Transactions on Power Systems, 33(6), 6410-6421.

[16] Bo, Z. Q., Lin, X. N., Wang, Q. P., Yi, Y. H., & Zhou, F. Q. (2016). Developments of power system protection and control. Protection and Control of Modern Power Systems, 1(1), 1-8.

[17] Strezoski, L., Padullaparti, H., Ding, F., & Baggu, M. (2022). Integration of utility distributed energy resource management system and aggregators for evolving distribution system operators. Journal of Modern Power Systems and Clean Energy, 10(2), 277-285.

[18] Cao, D., Hu, W., Zhao, J., Zhang, G., Zhang, B., Liu, Z., ... & Blaabjerg, F. (2020). Reinforcement learning and its applications in modern power and energy systems: A review. Journal of modern power systems and clean energy, 8(6), 1029-1042.

[19] Zhang, Y., Shi, X., Zhang, H., Cao, Y., & Terzija, V. (2022). Review on deep learning applications in frequency analysis and control of modern power system. International Journal of Electrical Power & Energy Systems, 136, 107744.

[20] Shen, J., Jiang, C., Liu, Y., & Wang, X. (2016). A microgrid energy management system and risk management under an electricity market environment. Ieee Access, 4, 2349-2356.

[21] Xiao, G., Xu, F., Tong, L., Xu, H., & Zhu, P. (2022). A hybrid energy storage system based on self-adaptive variational mode decomposition to smooth photovoltaic power fluctuation. Journal of energy Storage, 55, 105509.